Advances in Radiation Oncology (2024) 9, 101544

advances in radiation oncology

www.advancesradonc.org

Scientific Article

A Simulation-Free Replacement Solution for Radiation Therapy Immobilization Devices Using Computer Numerical Control (CNC) -Milled Polystyrene Molds

Samuel Hellman, PhD,[a,*,1] Laszlo Voros, MS,[a,1] Victoria Y. Yu, PhD,[a] Dale M. Lovelock, PhD,[b] Sean Berry, PhD,[a] Lei Zhang, PhD,[a] Margie Hunt, MS,[a] Joseph O. Deasy, PhD,[a] and Laura Cervino, PhD[a]

[a]*Department of Medical Physics, Memorial Sloan Kettering Cancer Center, New York, New York; and* [b]*Department of Radiation Oncology, Icahn School of Medicine, Mount Sinai Hospital, New York, New York*

Received 11 December 2023; accepted 2 May 2024

Purpose: In radiation therapy (RT), if an immobilization device is lost or damaged, the patient may need to be brought back for resimulation, device fabrication, and treatment planning, causing additional imaging radiation exposure, inconvenience, cost, and delay. We describe a simulation-free method for replacing lost or damaged RT immobilization devices.

Methods and Materials: Replacement immobilization devices were fabricated using existing simulation scans as design templates by computer numerical control (CNC) milling of molds made from extruded polystyrene (XPS). XPS material attenuation and bolusing properties were evaluated, a standard workflow was established, and 12 patients were treated. Setup reproducibility was analyzed postfacto using Dice similarity coefficient (DSC) and mean distance to agreement (MDA) calculations comparing onboard treatment imaging with computed tomography (CT) simulations.

Results: Results showed that XPS foam material had less dosimetric impact (attenuation and bolusing) than materials used for our standard immobilization devices. The average direct cost to produce each replacement mold was $242.17, compared with over $2000 for standard resimulation. Hands-on time to manufacture was 86.3 minutes, whereas molds were delivered in as little as 4 hours and mostly within 24 hours, compared with a week or more required for standard resimulation. Each mold was optically scanned after production and was measured to be within 2-mm tolerance (pointwise displacement) of design input. All patients were successfully treated using the CNC-milled foam mold replacements, and pretreatment imaging verified satisfactory clinical setup reproduction for each case. The external body contours from the setup cone beam CT and the original CT simulation with matching superior-inferior extent were compared by calculating the DSC and MDA. DSC average was 0.966 (SD, 0.011), and MDA average was 2.694 mm (SD, 0.986).

Conclusions: CNC milling of XPS foam is a quicker and more convenient solution than traditional resimulation for replacing lost or damaged RT immobilization devices. Satisfactory patient immobilization, low dosimetric impact compared with standard immobilization devices, and strong correlation of onboard contours with CT simulations are shown. We share our clinical experience, workflow, and manufacturing guide to help other clinicians who may want to adopt this solution.

Introduction

Modern radiation therapy (RT) uses immobilization devices for the treatment delivery of almost every patient.[1] Depending on the treatment site and treatment technique,

Sources of support: This work was funded in part through the NIH/NCI Cancer Center Support Grant P30CA008748.

Research data are stored in an institutional repository and will be shared upon request to the corresponding author.

[1]S.H. and L.V. contributed equally to this work.

*Corresponding author: Samuel Hellman, PhD; Email: hellmans@mskcc.org

https://doi.org/10.1016/j.adro.2024.101544

a wide variety of patient-specific immobilization and positioning devices are fabricated and used during computed tomography (CT) simulation and subsequent treatments to enable reproducible patient positioning on the flat tabletops used during treatment delivery throughout the treatment course. Although the flat tabletop allows repeatable setups and provides indexing features, it is neither comfortable for patients nor does it offer sufficient restriction against patient movement. Therefore, patient-specific immobilization devices have become a standard component of the safe and precise delivery of RT.[2,3]

During the course of clinical operations, immobilization devices may get lost (eg, misplaced, accidentally discarded, or lost in transit) or damaged (eg, punctured, torn, or deflated) and require replacement.[4] In hospitals with a large network, multiple treatment facilities, and/or a large number of patient transfers between sites, such events become increasingly likely. Although the size and complexity of our institution may yield more frequent occurrences, it is expected that this problem may exist in any radiation oncology department.

When a device requires replacement, the standard solution is a resimulation. This requires bringing the patient back for a full simulation, creation of new immobilization device, replanning, and completion of quality assurance procedures. For the patient, this is not only inconvenient but also may result in additional imaging radiation exposure and potentially disrupted or delayed treatment. For the clinic, this means additional cost in time and resources and additional strain on the entire care team. Alternatively, digital manufacturing for preparing a replacement mold without the need of resimulation may be used without the additional steps and lost treatment days.

Our institution has predominately used handmade immobilization devices for standard RT simulations, including custom-molded foams, reusable vacuum bags, thermoplastics, and custom-developed immobilization boards. We also use several standard commercial products. Recently, we started to introduce computer-aided manufacturing (CAM) for special clinical scenarios, including patient image-based immobilization (IBI) devices that can be computer numerical control (CNC)-milled, 3D-printed, or molded from digitally-based designs. The efficacy of in-house CNC-milled custom immobilization was previously validated in institutional feasibility studies where volunteers and patients underwent magnetic resonance simulation on a cushion without immobilization, and the simulation scan was used to accurately replicate the "space" between the flat tabletop and the patient's body using CNC-milled IBI molds made from extruded polystyrene (XPS).[5-7] The IBI molds were shown to achieve setup positioning shifts similar to those of standard-of-care handmade anterior thermoplastic immobilization fabricated during simulation.[5]

The use of a similar technique to replace a deflated vacuum bag was described for treatment in the right thigh.[8] In the present report, the suitability of the XPS material as a direct replacement is examined in more detail, and consideration for clinical implementation of the workflow, along with some clinical case examples, is discussed. This technique provides a rapid and reliable method for immobilization device replacement.

Methods and Materials

Patient acceptance criteria

Experience with 12 patients who benefited from mold fabrication is described. Given that the IBI mold immobilizes posteriorly, immobilization setups with head and neck thermoplastic masks are more challenging to replicate and, therefore, were excluded from the current study. To apply the replacement IBI mold fabrication process, we generated a guide and implemented a decision-making process that involved physicians, medical physicists, and radiation therapists. This team reviews every event and makes decisions on a case-by-case basis as to whether or not the IBI mold fabrication process can be used. Our RT technologists (RTT) managers are typically the first in line to get notified about lost/damaged immobilization devices. A simple acceptance criteria questionnaire specific to the treatment site and original immobilization setup (Table 1) was provided to the RTT team as a screening guide for the IBI mold replacement process. If initial criteria were satisfied, RTT managers contacted the clinician and informed the rest of the team (physics and IBI support team) for a case review. Collective decisions were made by the group as a whole based on patient clinical needs, complexity and dosimetry of the original treatment plan, feasibility of immobilizing with replacement, and required timeline/resources. The IBI replacement workflow is shown in Fig. 1.

IBI mold fabrication and verification

Replacement IBI molds were fabricated from existing patient scans to replicate the patient's position at the time of the simulation setup. The IBI molds were CNC-milled with the following steps:

1. A semiautomated Medical Identity Management (MIM) workflow (MIM Software) was created and used for immobilization device contour creation through the following steps:
   a. User selected the simulation CT scan as part of workflow input.
   b. A rectangular box contour with a lateral width of up to 50 cm, height (anterior-posterior) of up to

Table 1 Acceptance criteria precheck list provided to screen for image-based immobilization replacement mold option

1. Does the original immobilization require a thermoplastic mask covering the head/face?	Yes/No
If question 1 is Yes, a replacement mold cannot be made. Only continue if question 1 is No	
2. Is the original simulation scan available?	Yes/No
3. Is the original simulation scan acquisition less than 4 wks?	Yes/No
4. Is the original simulation scan long enough and has sufficient field of view to immobilize the treatment site and additional relevant body parts?	Yes/No
5. Is the original immobilization used for the simulation one of the below setups? (If so, check applicable)	Yes/No
• Thermoplastic for pelvis region only	☐
• Vacuum bag	☐
• Alpha cradle	☐
The replacement mold process can only be considered if questions 2-5 are all Yes.	

21 cm, and length (superior-inferior) matching that of the entire simulation scan was added. The box contour was positioned such that the minimum distance between the patient's posterior body surface and the mold's (box's) posterior surface was ≥4 cm (to ensure structural integrity).

c. An anterior extension of the body's outer contour was generated, and a simple Boolean operation of the rectangular box minus anteriorly extended body outer contour was applied. The anterior extension of the body outer was created to systematically prevent any potential undercut issues. Undercuts are horizontally recessed areas that cannot be machined by a vertical milling tool and would also prevent the patient's anatomy from sliding into the mold.

d. User was prompted to create additional markings, eg, isocenter and anatomic landmarks such as umbilicus with the 3D Brush tool laterally across the mold as needed.

e. The final immobilization device contour was saved directly in MIM and exported as a stereolithography (STL) file.

2. The exported STL file was saved in the patient's electronic health record along with the simulation documents. The STL file was reviewed with our in-house

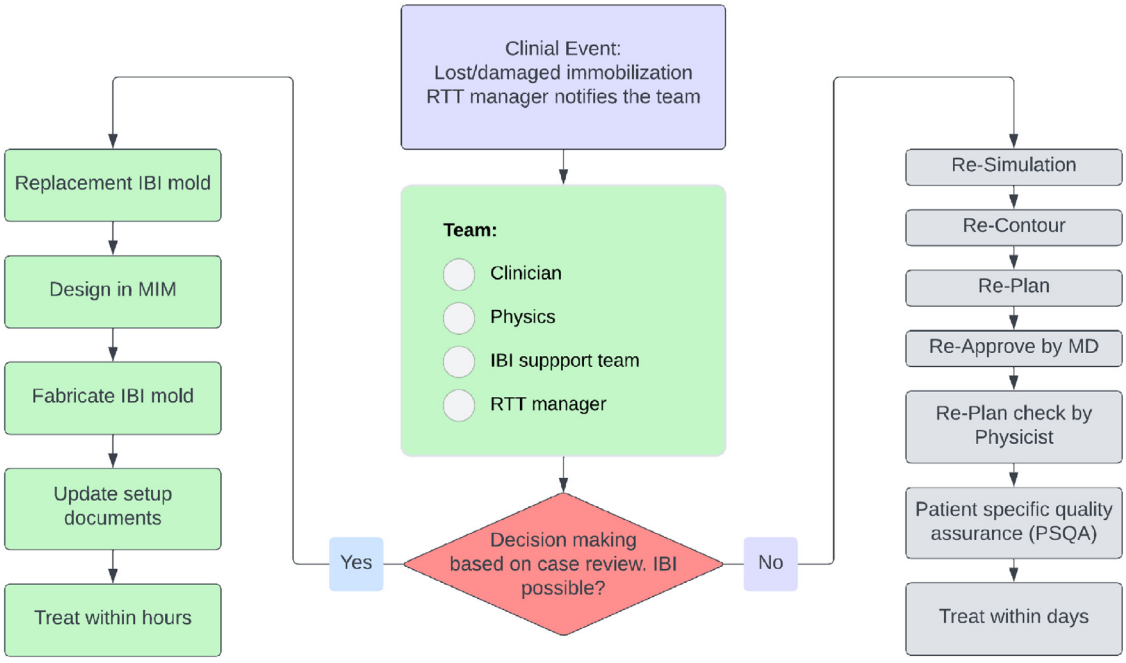

Figure 1 Flow chart of the image-based immobilization (IBI) replacement mold workflow.
Abbreviations: MIM = Medical Identity Management; RTT, radiation therapy technologists.

software, which can output the patient's name, orientation, and dimensions on the view to be saved into the setup documents for RTT reference when setting up treatment for patient.
3. The STL file was edited, if necessary. This included, eg, trimming extra material on the outside of molds to fit material blanks, reducing the number of facets on the STL to allow software processing, or removing unneeded areas after review with RTTs/physicians.
4. Blank blocks of 30 psi XPS foam (Radiation Products Design) were prepared by gluing together 7.2-cm sheets to the appropriate thickness using polyurethane glue. The sheets were clamped tightly together until cured to prevent gaps or excessive glue between layers.
5. The STL file was loaded into MeshCAM software (GRZ Software) to generate the CNC milling toolpaths.
6. The G-code was exported from MeshCAM, and the IBI mold was milled on a Laguna SmartShop II 3D CNC router (Laguna Tools). First, a roughing pass was carried out using a 1.58-inch, 6-flute, flat-end mill. The roughing pass (Fig. 2A) was performed in height-stepped, parallel toolpaths at a feed rate of 300 IPM and spindle speed of 6000 RPM. Next, the finishing pass (Fig. 2B) was performed with a 3D parallel toolpath using a 0.5-inch, ball-nose, burr end mill with the same feed rate and spindle speed.
7. Additionally, the posterior surface of the IBI mold was milled to allow fixation of the mold to the couch top (Fig. 2C). A set of channels and holes were milled in 5 cm increments to allow adjustable positioning of the device with the indexing bar that registers in the couch.
8. The IBI mold was cleaned using compressed air and then gently wiped with an acetone-damp rag to smoothen the final surface.
9. The finished IBI mold was labeled with appropriate patient information (name, MRN, date of birth and treatment location).

After fabrication, the IBI mold was optically scanned using an Artec EVA structured-light 3D scanner (Artec 3D). The captured 3D scan was compared with the input file to ensure that finished mold was within 2 mm (pointwise displacement) tolerance of design. The approximate time to plan and fabricate each mold was recorded along with material cost.

Each patient treated with an IBI mold underwent pretreatment imaging to ensure suitable position matching that of the simulation and treatment plan. The used imaging—either orthogonal kV films and/or cone beam CTs—adhered to institutional standard treatment protocols and criteria based on the treatment site, modality, and prescription for each case without modifications.

Material attenuation and bolusing

To ensure suitability of the XPS foam, dosimetric measurements were taken to compare the foam with immobilization device materials that are commonly used in our practice. The XPS foam was compared with samples of Alpha Cradle Form (Smithers Medical Products Inc), Vac-Lok Cushion (CIVCO Radiotherapy), and Gillfloor 5007C paneling (The Gill Corporation). The Alpha Cradle and Vac-Lok materials are commercially available solutions for patient immobilization, whereas the Gillfloor is a material used for in-house designed immobilization devices. The dimensions of the XPS test slab had a thickness of 7.2 cm $\pm$ 0.2 mm, whereas the Alpha Cradle and Vac-Lok test samples (because of less precise preparation process) were prepared to have a uniform thickness of approximately 7.2 cm $\pm$ 3 mm. These 3 materials are generally used in comparable thickness for patient immobilization. The Gillfloor sample was 0.4-cm thick because this is the thickness used for our in-house immobilization devices.

To measure attenuation of each material, a Farmer chamber was positioned at 10-cm depth, at isocenter, in a 30 cm $\times$ 30 cm $\times$ 30-cm solid water phantom. The field size was set to 15 cm $\times$ 15 cm, and measurements were taken for 6 MV and 15 MV photon beams. Percent attenuation was calculated as $100 \times (R_0 - R_S)/R_0$, where R_S is

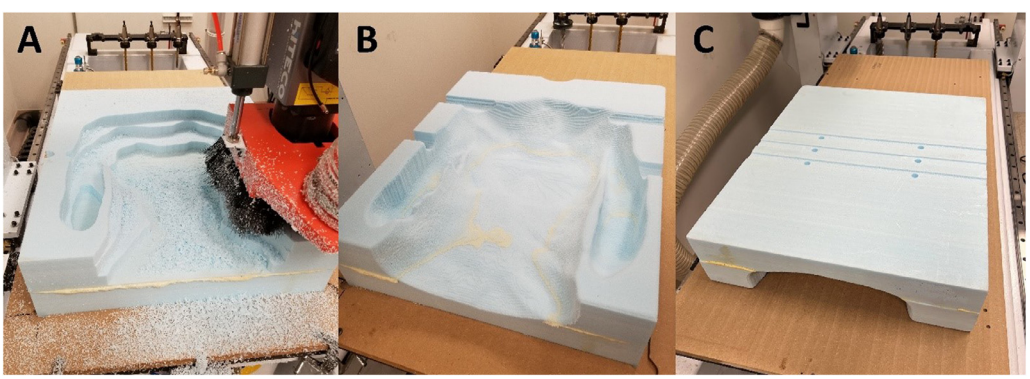

Figure 2 (A) Roughing pass of upper body posterior mold. (B) After finishing the pass. (C) Posterior surface of the mold with indexing bar channels/holes.

the electrical charge reading (in nC) with the sample placed on top of the phantom and R_0 is the reading without material sample in place.

The samples were also measured to evaluate the bolus effect of each material. Measurements were made using a parallel plate thin window chamber (Markus 34045) with a 0.9-mm cap. The proximal surface of the chamber was located on the central axis at isocenter with a field size of 15 cm × 15 cm, and measurements were taken for 6 and 15 MV photon beams at 100 MU. The increase in skin dose at 0.9 mm depth was calculated as $100 \times (R_S - R_0)/R_0$. All values were taken as the average of 2 consecutive readings, with no significant differences seen between subsequent measurements.

Contour overlap

For cases/sites with available full field of view onboard cone beam CTs (CBCTs) from the clinical setup with the custom molds, the external body contours from the setup CBCT and the original CT simulation with matching superior-inferior extent were compared by calculating the Dice similarity coefficient (DSC) and mean distance to agreement (MDA). DSC is a commonly used metric to describe the similarity of 2 samples—in this case, the extent of overlap between 2 imaging contours—with a value between 0 and 1 (0 indicating no overlap and 1 indicating perfect overlap).[9] MDA yields the average pointwise distance between the 2 contours.[10] Although these metrics were not used to make decisions on clinical applicability, DSC and MDA have been demonstrated as good quantitative measures of geometric similarity between contours.[11-13]

Results

IBI mold fabrication and verification

Over the course of 18 months, 12 IBI molds were created for 12 patients with a total of 14 treatment plans. The case details including treatment site, original immobilization, cause for device replacement, number of fractions, and time/resource to manufacture replacement mold are shown in Table 2. The labor time reflects approximate combined hands-on time for technician fabrication and planning time for physics. The mill time reflects the time that the CNC mill is operating to produce each mold. The total cost includes direct labor (based on average salary with overhead for technician and physicist time, respectively) and material costs but does not include any indirect depreciation or equipment costs. For 2 cases (cases 6 and 7), a single IBI mold was created to immobilize and treat 2 separate treatment sites. The average hands-on time was 86.3 minutes, and average cost was $242.17.

Figure 3 shows an example of the original device and replacement side by side, along with the device design. A wide variety of events resulted in the need for IBI replacement molds, which triggered different timelines and considerations in the IBI mold design and fabrication. The quickest turnaround from process initiation to delivery of replacement device to the treatment floor was within 4 hours (case 8). A wide range of treatment sites, patient positions, fractionation schemes, and plan complexity were successfully accommodated.

Aside from replacing the device and treating the intended treatment site as planned, additional treatment sites that were not initially planned were also safely accommodated without resimulation for 2 patients. Case 7 included 2 treatment sites that were initially immobilized with the same Alpha Cradle device but scanned in 2 different simulation scans, one foot-first and the other head-first. Simulation scans were long enough to create 1 device that could appropriately immobilize the 2 sites and replicate hip and lumbar spine flexion. With knowledge of the fact that both simulation scans used the same posterior device, image registration was performed in the overlapping regions of the 2 simulation scans to design a longer device spanning both scans. Case 12 allowed for treatment from an initial simulation scan for thoracic spine to an additional treatment in the ribs, which was not initially planned.

The replacement IBI workflow was also used to convert a 3D conformal treatment plan without immobilization to intensity-modulated RT to increase dose coverage to the bilateral neck for mediastinum disease while guaranteeing spinal cord sparing, requiring a more repeatable setup (case 10).

Given that the IBI mold replaces all devices between the patient's body and the tabletop, attenuation differences with or without an immobilization board had to be considered. In particular, CDR board (CDR Systems) attenuation has typically been considered as part of the treatment planning process at our institution by directly including relevant sections of the board directly into the external body contour for dose calculations. For cases in which IBI replacement was initiated after plan completion (case 7), plan recalculation and reapproval were required to remove the CDR board from dosimetric considerations. All other cases initially simulated with CDR board had the IBI replacement process initiated before treatment plan was created and, therefore, did not require additional plan modifications.

The IBI molds were all approximately 50 cm in width and ranged from 30 cm (cases 2, 5, and 9) to 90 cm (case 8) in length. The time required to mill each mold ranged from 43 to 125 minutes.

Based on the 3D optical scan results, each of the molds was measured to have less than 2 mm of total (surface

Table 2 Clinical case details for 12 cases undergoing treatment with replacement IBI molds

Case No.	Anatomic site	Original immobilization	No. of IBI fractions (of total fractions)	Cause for replacement	IBI mold fabrication resources
1	Lung	Q-fix and custom Alpha Cradle	30 (of 30)	Lost	Labor: 135 min Mill: 190 min MC: $124 TC: $364
2	Pelvis	Prostate board and thermoplastic	5 (of 5)	Lost	Labor: 75 min Mill: 70 min MC: $62 TC: $222
3	Clavicle	Lung board and Alpha Cradle	3 (of 3)	Lost	Labor: 75 min Mill: 120 min MC: $62 TC: $222
4	Breast boost	Vacuum bag (Vac-Lok)	4 (of 4)	Lost	Labor: 120 min Mill: 100 min MC: $62 TC: $282
5	Prostate	Prostate board and thermoplastic	26 (26)	Lost	Labor: 75 min Mill: 60 min MC: $31 TC: $191
6	Thoracic spine Lumbar spine	CDR board and Vac-Lok	5 (5)	Leaking vacuum bag	Labor: 90 min Mill: 165 min MC: $93 TC: $273
7	Lumbar spine Hip	CDR board and Alpha Cradle	1 (of 1) 3 (of 3)	Discarded early	Labor: 75 min Mill: 120 min MC: $62 TC: $222
8	Mediastinum	Q-fix and custom Alpha Cradle	6 (of 15)	Discarded early before cone down phase	Labor: 75 min Mill: 80 min MC: $62 TC: $222
9	Pelvis	Prostate board and thermoplastic	3 (of 3)	Lost	Labor: 75 min Mill: 65min MC: $62 TC: $222
10	Bilateral neck and Lung	No immobilization	1 (of 10)	Palliative anterior-posterior treatment converted to intensity-modulated radiation therapy	Labor: 90 min Mill: 120 min MC: $62 TC: $242
11	Thoracic spine	CDR board and Vac-Lok	5 (of 5)	Leaking vacuum bag	Labor: 75 min Mill: 120 min MC: $62 TC: $222
12	Rib	Q-fix and Vac-Lok	5 (of 5)	Discarded early, additional new treatment site	Labor: 75 min Mill: 120 min MC: $62 TC: $222

Abbreviations: IBI = image-based immobilization; MC = material cost; TC = total cost.

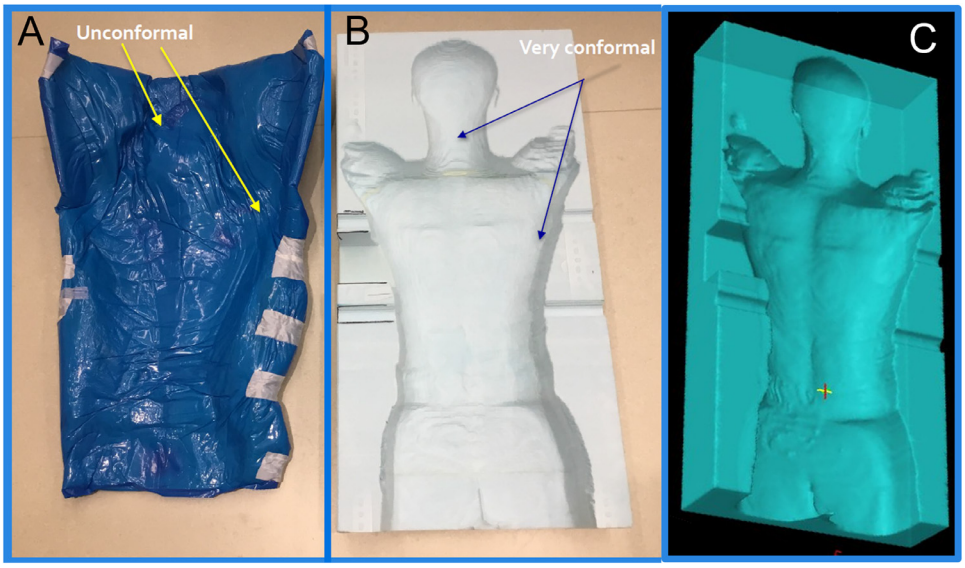

Figure 3 (A) Original Alpha Cradle, (B) replacement image-based immobilization mold, and (C) stereolithography design of mold for mediastinum treatment (case 8).

normal) displacement relative to the design input file at every point throughout the patient contour surface and mold posterior. An example scan is shown in Fig. 4. There were displacement errors of larger than 2 mm on the lateral and anterior surfaces of the molds; however, these were not milled areas and did not affect either patient positioning or indexing to the treatment tabletop.

Additionally, for all 12 patients and a total of 97 delivered fractions, pretreatment imaging per standard prescribed image-guided RT (orthogonal KV films and/or CBCT) was acquired to confirm patient and target alignment. All on-treatment imaging results were used to perform qualitative clinical assessments on target alignment, surrounding organs at risk, and external body contour agreement with the clinical treatment plan per institutional standards based on case complexity and were deemed clinically acceptable by RTTs, medical physicists, and attending physicians and proceeded smoothly to treatment without interruptions. Patient intrafractional motion was monitored either by surface-guided system or intrafraction motion review in the cases for which on-treatment monitoring was prescribed. CBCT to simulation CT overlay demonstrating the high level of setup consistency with the replacement IBI molds is shown in Fig. 5 for 3 example cases. Anatomy was well aligned between the scans, and external contour of the simulation scan showed good conformity to the CBCT for all cases.

Material attenuation and bolusing

Table 3 shows transmission results for the tested materials. The XPS foam had the lowest percentage attenuation and bolusing of all materials for both 6 and 15 MV photon beams. These results indicate that the XPS foam was indeed suitable as a replacement

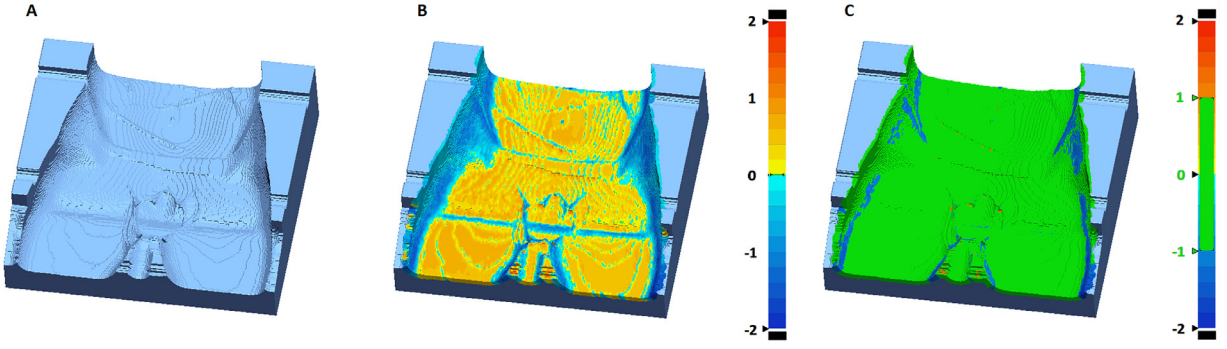

Figure 4 (A) Stereolithography design of a pelvic image-based immobilization mold for prostate treatment. (B) Scalar map showing discrepancy (displacement normal to surface in mm) at each point between the 3D scan of the final mold and the original design. (C) Same as (B), with a green overlay for all areas with <1 mm of discrepancy.

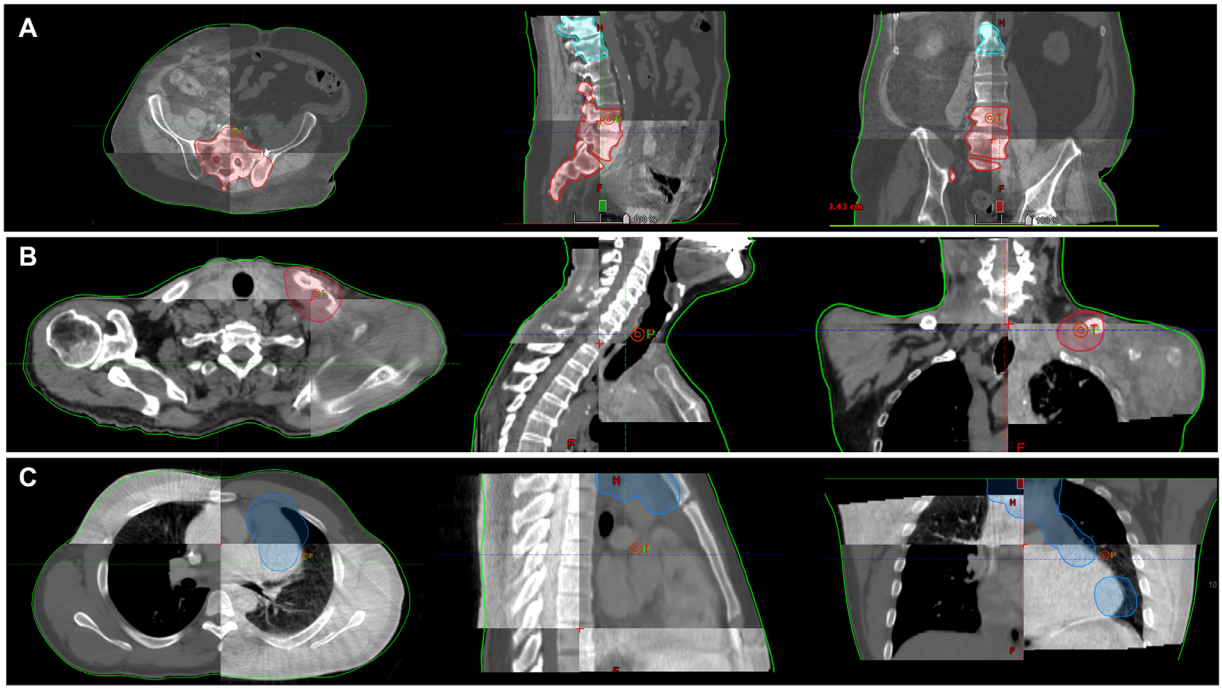

Figure 5 Simulation computed tomography (CT) with original immobilization overlaid with onboard cone beam CT using an image-based immobilization mold in axial, sagittal, and coronal views. Cone beam CT with image-based immobilization mold: top left and bottom right; planning CT with original immobilization: top right and bottom left. Green contour: external body contour on planning CT. (A) T12-L1 spine (Cyan) and lumbar to sacral spine (Red) 40 Gy in 5 fractions stereotactic body radiation therapy treatments with a small gap between the 2 sites. Corresponding to case 6 in Table 2. (B) Clavicle (Red) 30 Gy in 3 fractions of stereotactic body radiation therapy. Case 3 is in Table 2. (C) Mediastinum (Blue): 30 Gy in the 15 fractions convention. Case 8 is in Table 2.

material for immobilization devices and, in fact, had less dosimetric impact than other materials used in standard RT practice.

Contour overlap

Table 4 shows the DSC and MDA for 11 case sites that had full field of view onboard CBCTs from the clinical setup available. The average DSC was 0.966 (SD, 0.011), and average MDA was 2.694 mm (SD, 0.986). Although these metrics were not used for analyzing clinical suitability for each case, the DSCs indicate an excellent body contour agreement between the clinical treatment setups using the IBI molds and the CT simulators from which they were designed.

Discussion

It was demonstrated that IBI mold fabrication can be incorporated into the clinical workflow as a safe and suitable replacement solution for standard immobilization devices. This workflow allowed for elimination of patient resimulations (and associated extra imaging dose) and replanning while still providing clinically acceptable treatment delivery accuracy and patient comfort. For all IBI molds, quality check comparisons between the finished mold and the design input files showed that the fabrication process was successful. Through this study—and in other applications within our institution—we have found that the XPS foam holds up well to transportation and clinical use over repeated fractions. Additionally,

Table 3 Percent attenuation and bolusing of each material for 6 and 15 MV photon beams

Material	6 MV Attenuation (%)	15 MV Attenuation (%)	6 MV Bolusing (%)	15 MV Bolusing (%)
Extruded polystyrene foam	0.9	0.6	46.7	55.2
Alpha Cradle Form	1.6	0.9	62.5	78.0
Gillfoor 5007C	1.3	0.9	70.7	102.8
Vac-Lok Cushion	2.0	1.4	80.3	108.4

Table 4 Dice similarity coefficient and mean distance to agreement for 11 case sites

Case No.	Mean distance to agreement (mm)	Dice similarity coefficient
2	2.734	0.963
3	1.364	0.975
5	4.580	0.945
6	3.123	0.972
7 (site 1)	1.639	0.974
7 (site 2)	2.242	0.963
8	1.646	0.981
9	3.708	0.954
10	3.535	0.957
11	2.470	0.968
12	2.592	0.973
Mean	2.694	0.966
SD	0.986	0.011

postfacto analysis of the setup reproducibility using DSC and MDA showed that the IBI molds yielded onboard patient imaging contours with a high level of correlation to CT simulations. DSCs between 0.8 and 1 indicate a strong correlation, and results showed a minimum DSC of 0.954 (case 9), with an average of 0.966.

Our institution has a wide variety of patient positioning systems used for different sites and techniques, and each case presented varying levels of complexity. For example, an intensity-modulated RT treatment—immobilized with either a thermoplastic mask or vacuum bag—can be easily and safely substituted with an IBI mold. However, a stereotactic body RT treatment of an upper thoracic or cervical spine case—which may require rigid immobilization and usually includes a custom indexed vacuum bag and thermoplastic face mask—might need further careful consideration.

We were able to successfully setup many plans that require a high level of precision, including a single fraction lumbar spine treatment (case 7) as well as a 2-site lower thoracic to lumbar spine plan (case 6) with less than 1 cm gap between the 2 treatment volumes. Additional care in plan dosimetry was needed based on the original immobilization device (eg, any case with CDR board). The fact that the design of the device could be simply based on a contour allowed for a lot of flexibility in accommodating a range of treatment sites and treatment positions with replacement IBI molds.

The convenience and significant time/cost savings for patients, clinicians, and clinical care team have proven to be extremely valuable. A resimulation typically requires at least 1 week, whereas the IBI mold replacement process was completed in as little as 4 hours and typically in less than 24 hours. Thus, the elimination of resimulation for these patients avoids significant delays in treatment start. It was found that the average direct cost (material and labor) to produce a replacement mold was $242.17 and required an average of 86.25 minutes of hands-on time (110.8 minutes of milling time). Although a full cost analysis is beyond the scope of this study, the resimulation and planning for, eg, a 3D image-guided RT case, would typically cost our hospital more than $2000. This indicates that the IBI mold solution provides significant cost savings in addition to saving extra patient visits, radiation exposure, and staff/resource use.

The most unique elements of this process are the CNC router and a dedicated team with expertise in operating and implementing it because these resources are not commonly part of radiation oncology departments. Although some institutions will have the resources to put these systems in place, others may take advantage of academic partners or employ services from external US Food and Drug Administration-compliant companies that are able to support radiation oncology teams with custom-made devices. As digital planning and onsite manufacturing become increasingly important parts of personalized medicine, we believe that these types of capabilities will have increasing adoption in hospitals. Although we purchased the CNC router specifically for IBI molds (and not just replacement cases), it is worth noting that we have found many other clinical uses for this resource as well. We have also deployed the CNC router with foams, wax, wood, plastics, etc, eg, for making molds to cast silicone boluses, routing components for custom surgical fixtures and limb holding devices, making and modifying radiation shielding setups, and many others.

We found that it is important to communicate the basics of the manufacturing process with the treatment planning team to improve efficiency. For example, the XPS foam sheets we use are 7.2-cm thick, so a planner can take this into account when deciding the final height of an IBI mold, eg, selecting 14.4 cm—2 layers—rather than 14.5 cm, which would require a third layer and add only 1-mm thickness. Additionally, our router and tool combo will allow a maximum milling depth of around 21 cm, so any IBI mold taller than this requires fabricating pieces in multiple operations and aligning/gluing them together afterward, which adds significantly to mold delivery time and labor. It is beneficial to standardize as much as possible for efficient workflows; for example, we use 50-cm width for molds whenever appropriate because this allows us to prepare and have standardized blanks on hand. Finally, it is important to consider proper facilities and material handling when milling foam. A powerful dust collection and filtration system along with proper personal protective equipment are required for safety. Additionally, a foam densifier (either mechanical or thermal) allows for compressing the volume of foam

approximately 90:1 to facilitate recycling of shavings and molds after use.

These results have a few limitations. The nature of the proposed workflow as a replacement/backup strategy precludes generalizability among the included cases. Therefore, it was difficult to quantitatively and systematically compare setup performance between the original immobilization device and IBI molds. However, previous preclinical work has quantitatively indicated good reproducibility,[5] whereas in the presently reported cases, we were able to demonstrate that all setups satisfied clinical suitability for treatment delivery. In addition, setups requiring head and neck anterior thermoplastic masks were excluded from this workflow because we determined that the level of immobilization provided by anterior masks for the required rotations and flexions could not be matched by posterior immobilization alone. However, we have shown in several example cases that posterior immobilization with IBI molds from the head continuously down to the torso can be well reproduced and is consistent with treatment alignments. Recreation of anterior immobilization masks on top of the IBI molds with appropriate fastening mechanisms or heightened intrafractional motion monitoring of the face with surface-guided systems could be considered.

Although the clinical application of replacement immobilization may be relatively limited in scope across hospital networks, it is also a relatively high-impact area because of the time, stress, and radiation exposure spared for patients. Furthermore, it is anticipated that the prevalence of this issue is underreported. Within our own institution, the frequency of requests has gone up significantly since the completion of our study, and providers were made aware of this solution. In addition to the impact of this study on replacement of immobilization, it demonstrates the viability of the technique for regular clinical use and expansion into standard workflows.

In future work, IBI fabrication for diagnostic CT-based (simulation-free) palliative treatments will be further explored. A diagnostic CT-based plan in combination with an IBI mold could potentially serve as a base plan and immobilization device for on-couch adaptive planning workflows. Such efforts could result in impactful reduction in time needed between simulation and treatment.

Conclusions

A new workflow is described for replacement of lost or damaged immobilization devices used in RT. This workflow eliminates the need for resimulation and reduces patient exposure to additional radiation, inconvenience, cost, and delay. The replacement devices are created from existing simulation scans and fabricated using CAM technology, specifically CNC-milled molds made from XPS. The article outlines the advantages of using CAM technology over the traditional handmade replacement approach and reports on preclinical tests for material dosimetric properties, fabrication process, quality control, and clinical implementation of this technique on 12 patients. Results show that this technique provides a rapid and reliable method for immobilization device replacement and can serve as a potential backup procedure for immobilization device replacement in RT departments and clinics with high-impact time savings. This study demonstrates the clinical viability of the process for replacement and that it may be suitable as a standard workflow for immobilization in the future—potentially enabling simulation-free treatment planning.

Disclosures

Dale M. Lovelock reports holding a related patent on systems and methods for designing and manufacturing custom immobilization molds for use in medical procedures. US Patent No. 11568618, 2023. Available: https://patentimages.storage.googleapis.com/0f/50/eb/eed4af4254169f/US11568618.pdf. Joseph O. Deasy reports holding a related patent on systems and methods for designing and manufacturing custom immobilization molds for use in medical procedures. US Patent No. 11568618, 2023. Available: https://patentimages.storage.googleapis.com/0f/50/eb/eed4af4254169f/US11568618.pdf. The remaining authors declare no conflicts of interest. Clinical cases reported under this research fall under the practice of medicine. The included patient images, from examinations performed between January 2021 and September 2023, were analyzed retrospectively under Memorial Sloan Kettering Institutional Review Board protocol #16-1488.

References

1. Hoskin P. *External Beam Therapy (Radiation therapy in Practice).* 3rd ed. Oxford University Press; 2019.
2. Verhey LJ, Goitein M, McNulty P, Munzenrider JE, Suit HD. Precise positioning of patients for radiation therapy. *Int J Radiat Oncol Biol Phys.* 1982;8:289-294.
3. Saw CB, Yakoob R, Enke CA, Lau TP, Ayyangar KM. Immobilization devices for intensity-modulated radiation therapy (IMRT). *Med Dosim.* 2001;26:71-77.
4. Metzger A, Renz P, Hasan S, Karlovits S, Sohn J, Gresswell S. unforeseen computed tomography resimulation for initial radiation planning: associated factors and clinical impact. *Adv Radiat Oncol.* 2019;4:716-721. 20.
5. Voros L, Yu V, Hellman S, et al. Using image-based immobilization devices for prostate patients receiving radiation therapy with treatment plans derived from MR-simulation. *Presented at: the American Association of Physicists in Medicine (AAPM) Annual Meeting.* Hoboken, NJ; Jun 1, 2020.

6. Voros L, Yu V, Zhang L, et al. Have you lost your mold during the COVID-19 Pandemic? *Medical Physics*. 2022:E460.
7. Booth P, Lee N, Lovelock D, et al. A feasibility study of computer milled immobilization cradles for head and neck radiation therapy. *Presented at: 59th Annual Meeting and Exhibition of the American Association of Physicists in Medicine (AAPM)*. Denver, CO; 2017.
8. Gensheimer MF, Bush K, Juang T, et al. Practical workflow for rapid prototyping of radiation therapy positioning devices. *Pract Radiat Oncol*. 2017;7:442-445.
9. Evans JD. *Straightforward Statistics for the Behavioral Science*. Pacific Grove: Thomson Brooks/Cole Publishing Co; 1996.
10. Jena R, Kirkby NF, Burton KE, Hoole AC, Tan LT, Burnet NG. A novel algorithm for the morphometric assessment of radiotherapy treatment planning volumes. *Br J Radiol*. 2010;83:44-51.
11. Gooding MJ, Smith AJ, Tariq M, et al. Comparative evaluation of autocontouring in clinical practice: A practical method using the Turing test. *Med Phys*. 2018;45:5105-5115.
12. van der Veen J, Willems S, Deschuymer S, et al. Benefits of deep learning for delineation of organs at risk in head and neck cancer. *Radiother Oncol*. 2019;138:68-74.
13. Heimann T, van Ginneken B, Styner MA, et al. Comparison and evaluation of methods for liver segmentation from CT datasets. *IEEE Trans Med Imaging*. 2009;28:1251-1265.